


**Research Article**

Graphene-based stand-alone nanomechanical membrane production and mass-acoustic hybrid-sensor application

Gorkem Memisoglu ^{a,b,*} 

^aIstiklal University, Electronics Technology Program, 46100-Kahramanmaraş, Türkiye

^bUniversidad del País Vasco/ Euskal Herriko Unibertsitatea-UPV/EHU, Electronics and Communication Engineering Department, 48013-Bilbao, Spain

ARTICLE INFO*Article history:*

Received 06 January 2023

Accepted 30 May 2023

Published 15 August 2023

Keywords:

Graphene;

Graphene preparation;

Graphene-based membrane fabrication;

Hybrid nanomechanical membrane sensor chip.

ABSTRACT

In this article, experimental studies were carried out for the preparation, characterization, and nanomechanical membrane application of Graphene-based nanomechanical mass and acoustic hybrid sensors. The purpose of this study was to prepare facile and low-cost nanomechanical membrane-based mass-acoustic hybrid sensors by set-ups developed on the exfoliation and membrane transfer methods, and to examine their morphological, spectroscopical, and nanomechanical-vibrational properties, as well as the membrane characteristics like mass and acoustic sensitivities and durability over time. For the experiments, equipment and items such as optical, digital, atomic force and scanning electron microscopes, Raman spectroscopy, acoustic signal source and amplifier, data-logger, sound pressure level meter, and laser Doppler vibrometer were used. Graphene-based nanomechanical membrane sensor chips with varying acoustic pressure levels and mass-loadings were tested. It was observed that the acoustic sensitivity of the produced $706.5 \mu\text{m}^2$ nanomechanical membranes increased with increasing sound pressure levels and decreased with increasing mass-loads. With $67.8 \pm 5 \text{ nm/Pa}$, the unloaded nanomechanical membrane was the most sensitive sample. Experimental challenges and sensor development solutions were discussed. Existing application examples were examined and discussions were made on the current challenges and the future prospects of the nanomechanical membrane sensors.

1. Introduction

Graphene is a valuable nanotechnological material with excellent mechanical, optical, electrical, and chemical properties. It has been extensively researched since its discovery in 2004 and can be found in many areas of our lives [1–5]. Graphene has many important properties such as easy adaptation to nanoscale, ultra-light weight, planar, mechanically flexible and ultra-strong structure, large specific surface area, antimicrobial activity, and biocompatibility that can be valuable for biological applications. This material, which is stronger than steel, exhibits an elastic (Young) modulus of about 1 TPa, resonates between kHz and THz frequencies, and promises not only nanoscale precision design but also high performance in mechanical, electrical, chemical, and physical systems [6–10]. Features exhibited by Graphene-based membranes (GMs) make them appropriate materials

for nanomechanical systems capable of sensing acoustic stimulation/vibration, mass, position, temperature, pressure or applied force [1,2].

A membrane is a single or multi-layered element consisting of planar structures in various geometries (like circular or square), which can be suitable for vibration when an external effect is applied. Membrane properties vary depending on the raw materials in its structure. The graphene membrane was prepared for the first time in 2007 to use as a resonator at MHz frequency in nanomechanical systems [1]. Today, GMs are used in many areas from sensors to mechanical switches [11–16].

Low hardware complexity, room temperature operation, or audio signal transmission capability are some advantages of Graphene-based nanomechanical membranes (GNMs) [12]. In addition, GNMs provide benefits for both control and wireless communication or power transmission in nanomachines. For example, Graphene-based THz

* Corresponding author. Tel.: +90(344)400-10 00.

E-mail addresses: gorkem.memisoglu@istiklal.edu.tr, gorkem.memisoglu@ehu.eus (G.Memisoglu)

ORCID: 0000-0002-3229-6702 (G.Memisoglu)

DOI: [10.35860/iarej.1230632](https://doi.org/10.35860/iarej.1230632)

© 2023, The Author(s). This article is licensed under the CC BY-NC 4.0 International License (<https://creativecommons.org/licenses/by-nc/4.0/>).

magneto-inductive wireless communication/power transmission provides 10^3 times higher power efficiency in harsh environment by reaching several Tbit/s (10^{12} bit/s) compared to conventional RF and optical or molecular communication systems with ground-breaking theoretical performances [17–19]. Moreover, Graphene-based systems can provide ultra-low power (500×10^{-21} J/bit) channel efficiency (10^7 times higher than state-of-the-art) and efficient power transfer in the range of a few millimeters (10^9 W/mm²) [17–19].

Figure 1 shows the timeline for some selected Graphene-based discoveries such as Graphite discovery (1500s), Graphite layering (1840), Graphene oxide discovery (1859), Graphene discovery (2004), and for some applications such as GNMs, stethoscopes or acousto-optical actuators. In the literature, there are some purely Graphene design studies such as Graphene switches [15,20] or Graphene-based supercapacitors [16,21] constructed with Graphene membranes and Graphene coils that can provide a unique set of matched components for advanced quantum nanomachines [15,16,20,21]. In the last five years, nanoparticle-coated nanomechanical sensor arrays have been used for quantitative odor analysis [22]. In references [9,23], acousto-optic systems using Graphene membranes were designed and tested. Electron acceptor material was placed on a silicon dioxide (SiO₂) substrate/Graphene surface, and electron donor material was placed on another substrate/Graphene surface. In the aforementioned study, a system in which the donor and acceptors were joined face to face with a nanometric distance between them was created. The system structure from top to bottom was in the form of SiO₂/Graphene/donor-gap-acceptor/Graphene/SiO₂. In such systems, donor materials absorb the light energy to give it to the nearest acceptor materials non-radiatively (non-radiative energy transfer while the distance between the donor and acceptor is less than 10 nm by the help of the vibration of the Graphene membrane), which results in the light emission of acceptor materials. It has been reported that the membrane vibration plays a significant role in the performance of this system, as great as the characteristics of the donor and acceptor materials used.

GNMs can be vibrated by external stimulations like electrostatic signals [1,24], electrical signals [2], mechanical thrust [25], or acoustical signals [26]. The external stimulations can help the adjustment of the membrane deflection level in the nanometer or micrometer scales [1,2,24,27,28].

Thanks to their sensitivity to mass, force, strain, acceleration, pressure or acoustic signals that make them find usage area in chemical or biological process control - particle tracking in micro-fluidics in healthcare applications, or surface science events like diffusion, NMs attract attention [29-45].

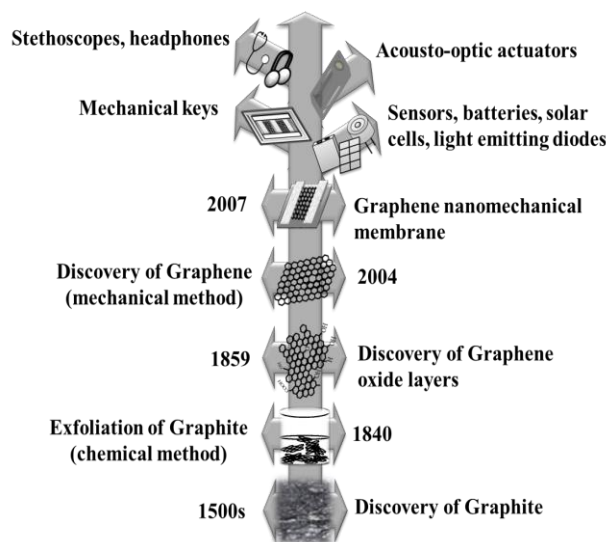


Figure 1. Timeline for Graphite, Graphene oxide, Graphene and Graphene nanomechanical membrane discoveries, and some selected Graphene-based applications.

In an ideal nanomechanical mass sensor, a large sensing surface area or high mass sensitivity can be shown among the important features. Recently, many efforts have been made to produce sensors made of Carbon nanostructure materials like Graphene. Thanks to their high surface area and nanomechanical vibration characteristic, GNMs have higher elastic modulus and greater surface-to-volume ratio, and they can detect lower mass-load or applied pressure compared to the conventional NMs. Table 1 shows the structures of GNM sensor chip devices, their main properties, and application areas [1,2,5,9,12-14,24,28–32,35,38,42-45]. In the last 3 years, GNMs have been used in many applications such as mass sensor [5], point-of-care application [9], gas detection [13], microphone application [14], environmental monitoring [28], current sensing [29], thermal stress sensing [30], or pressure sensing [45]. From mass sensing to particle tracking applications, generally all membranes can act in accordance with Newton's laws of motion. Some of the important parameters in membranes are the Young's modulus (elasticity that is related to the stress and strain according to the Hooke's law) [34], vibration amplitude (deflection) [11], vibration frequency, sensitivity, and mass responsivity [35].

Regarding the membrane vibration amplitude (deflection amount of membrane) for the varying pressure difference between two surfaces (top and bottom of the membrane), the pressure difference between these surfaces (ΔP) can be expressed by the following equation [11]:

$$\Delta P = \frac{4z}{\omega^2} \left(c_1 S_0 + \frac{4c_2 E t z^2}{\omega^2 (1 - \nu)} \right) \quad (1)$$

where z is the deflection, t is the thickness, ω is the width, E is the elastic modulus (1 TPa), S_0 is initial tension per

unique length, ν is the Poisson ratio (0.16), and c_1 and c_2 are equal to 3.393 and $(0.8 + 0.062 \nu)^{-3}$.

In terms of using the membrane in specific application, vibration frequency of it is important. For instance, GMs can vibrate at the kHz - MHz frequencies and this can be helpful for using them in multiple-particle tracking in micro-fluidic environments in healthcare applications [26,32]. Considering the membrane vibration frequency, the following equation is used to calculate the membrane mass [35]:

$$m_{attached} = \alpha \left(\left(\frac{f_{withoutmass}}{f_{withmass}} \right)^2 - 1 \right) \quad (2)$$

where $m_{attached}$ is the attached mass (loaded mass), $f_{withoutmass}$ is the vibration frequency of pristine membrane (without mass load), and $f_{withmass}$ is the vibration frequency of membrane with mass load.

The vibration frequency of a pristine membrane can also be expressed by the following equation [36]:

$$f_{withoutmass} = \frac{\alpha_{i,j}}{2\pi r} \sqrt{\frac{T}{\rho t}} \quad (3)$$

where α_i is a dimensionless parameter (for the first fundamental (0,1) mode, $\alpha_{i,j}$ is 2.405, r is membrane radius (μm), T is membrane tension (N/m) with $i, j = 0, 1, 2, \dots$, ρ is membrane density (kg/m^3), and t is membrane thickness (m).

NM mass sensor sensitivity (δ_{mass}) can be defined as the differential frequency change per mass change in the center of the membrane surface. Additionally, it is also equal to the minimum mass value needed to induce a specified frequency shift in the sensor. Therefore, the mass sensitivity of a membrane can be defined as in the following equation [35,37]:

$$\delta_{mass} = \left(\frac{2m_{effective}}{f_{withoutmass}} \right) \delta_{mass} f_{withoutmass} \quad (4)$$

where $m_{effective}$ is the effective mass and $\delta_{mass} f_{withoutmass}$ is the standard deviation of the measured frequency. Graphene-based nanomechanical mass sensors present high sensitivity ($\sim 10^{-21}$ g even when operated at cryogenic temperature) [2,38,39]. In addition, mass responsivity (R_{mass}) is a quantity that is related to the effective mass and vibration frequency of the pristine membrane (without mass load), as can be described with the following equation [35]:

$$R_{mass} = (2m_{effective}/f_{withoutmass})^{-1} \quad (5)$$

The main problem related to detecting very low mass at room temperature in air is to measure the small amount of deflection changes with the maximum possible precision. Additionally, ultra-sensitive measurement of membrane sensitivity to human hearing frequency under normal conditions is another important issue. In this study,

deflection tests were performed to use the suspended many-layer Graphene chips as NMs in micron-width mass and acoustic sensors. The improvable performance parameters such as the sensitivity of mechanically exfoliated NMs were presented in this study.

The creation of low-dimensional hybrid sensors by using graphene, along with detailed characterizations can be represented as the contribution of this study to the literature. Moreover, in this study, the experiment results were also examined taking into account device sensitivity and durability while considering current challenges and future prospects.

2. Materials and Methods

Raw materials, chemicals and materials used in the experiments were Graphite flakes (1 mm diameter), quantum dots (6 nm diameter Cadmium Sulphide (CdS)), pure-water, de-ionized water, detergent, acetone, iso-propanol, toluene, silica gel, poly-dimethyl siloxane, SiO₂ frame-substrates, and adhesive tape (Nitto, Scotch and 3M).

Some of the tools and equipment used during the preparation of Graphene and membranes were electronic pipette, pipette tip, compressed-air gun, micromanipulator and desiccator. However, instruments and equipment used in Graphene membrane characterizations were optical microscope (Leica), digital microscope (Dinolite), atomic force microscope (Bruker), scanning electron microscope (Jeol), Raman spectroscopy (Renishaw Raman), acoustic source (works between 20 Hz and 20 kHz frequency range) (Thorlabs), data collector (data-logger), signal amplifier, sound pressure meter (SPL-meter), and laser Doppler vibrometer (Polytec).

In the experimental stage, firstly, Graphene layers were prepared by the mechanical (physical) exfoliation method, which is facile, low-cost, and environmentally friendly, without requiring a vacuuming, chemical gas, or an extra anchoring-stabilizing layer addition [4,9,40,41]. The Graphite layers were mechanically exfoliated into the Graphene layers through a developed semi-automatized exfoliation set-up (Figure 2(a)), in which a press roller-iron rod was manually moved between the two blocks to perform the mechanical exfoliation by using the adhesive tapes called Nitto, 3M, and Scotch-tape.

Many layer Graphene samples obtained after the exfoliation process were transferred onto the SiO₂ frame-substrates with 30 μm width circular hole by using the soft-wet transfer technique. Before the transfer process, the frame-substrates were cleaned: after cleaning with detergent-pure water mixture, they were kept in distilled water, acetone and finally in iso-propanol for 15 minutes at each step in the sonication device.

Table 1. Structures, main properties, and application areas of the selected nanomechanical membrane-based device.

Ref #	Device structure	Main properties	Application area
Ours	SiO ₂ /Graphene, SiO ₂ /Graphene/CdS	Membrane motion by applied acoustic signals and mass-load. Highly sensitive, durable 30 µm width membranes vibrated in kHz frequencies.	Mass and acoustic sensor
[1]	Si/SiO ₂ /Graphene/Gold	Electromechanical membrane motion in MHz.	Mass and force sensor
[2]	Si/SiO ₂ /Graphene/Gold	Membrane motion in MHz by applied voltage.	Mass sensor
[13]	Si/Graphene oxide	Sensor operation in static mode.	Gas and surface stress sensor
[24]	Si/Graphene/Chrome/Gold	Electro-static membrane motion.	Signal processing
[29]	Ceramic ferrule/Gold/Graphene	Nano-opto-mechanical membrane motion.	Current sensor
[30]	Ceramic ferrule/Gold/Graphene	Nano-opto-mechanical membrane motion.	Thermal stress sensor
[31]	Si/SiO ₂ /Graphene/Chromium/Gold	Nano-electro-mechanical membrane motion.	Single atomic mass sensor
[28]	SiO ₂ /Graphene/CdSeDonor/ZnS/Gap/ CdSeAcceptor/ZnS/Graphene/SiO ₂	Förster resonance energy transfer and membrane motion by applied acoustic signals.	Acoustic sensor
[38]	Si/SiO ₂ /Graphene/Gold	Nano-electro-mechanical membrane motion.	Biomedical sensor (glucose sensor)
[42]	Si/SiO ₂ /Graphene/Gold	Nano-electro-mechanical membrane motion.	Pressure sensor
[9]	SiO ₂ /Graphene Oxide/CdTe, SiO ₂ /Graphene/CdTe	Förster resonance energy transfer and membrane motion by applied acoustic signals.	Acoustic sensor
[25]	Ceramic ferrule/Graphene	Nano-opto-mechanical membrane motion.	Pressure sensor
[32]	SiO ₂ /CdSe-ZnS/Gap/CdSe-ZnS/ Graphene/SiO ₂	Förster resonance energy transfer and membrane motion by applied acoustic signals.	Optical modulator
[43]	SiO ₂ /Graphene/Molecular magnet	Magnetically membrane motion.	Wireless communication and power transfer
[26]	SiO ₂ /Graphene/CdSe/ZnS	Membrane motion by applied acoustic signals.	Optical nanoscale radar and particle tracking
[14]	SiO ₂ /Graphene (chemical etching was used while suspended membrane preparation)	Membrane nanomechanical motion by applied acoustic signals. Clamped 85-300 µm diameter membranes. 92 nm/Pa acoustic sensitivity.	Microphone
[35]	Graphene/Carbon nanotubes	Nanomechanical membrane motion. 1 yg mass sensitivity.	Mass sensor
[44]	Silicon nitride/Graphene	Nano-electro-mechanical membrane motion.	Nano-electro-mechanic resonator
[45]	Ceramic ferrule/ Graphene/Gold	Nano-opto-mechanical membrane motion.	Gas and pressure sensor
[12]	Si/Graphene/Gap /SU-8 polymer/Metal	Membrane motion by applied electrostatic signals at room temperature.	Graphene membrane as oscillator and frequency mixer
[5]	Si/SiO ₂ /Graphene/Gold	Nano-electro-mechanical membrane motion.	Mass sensor

Then, the substrates were dried with a compressed air-gun, and finally they were kept in a vacuum oven for 15 minutes at 100 °C. Just before the Graphene membrane transfer process, to improve the contact between the substrate and the membrane, possible dust was first removed by a compressed air-gun, and then, molecular impurities on the substrate surface were removed by an oxygen-plasma under vacuum for 5 minutes.

In the mechanical exfoliation of Graphite, the adhesive strength of the adhesive tape and the amount of manual pressure are important to achieve similar results every time with each parallel step [4,9,40,41]. For this method, the set-up of a mechanical exfoliation mechanism consisting of two block surfaces, a press roller, and an iron bar was developed.

Figure 2(a) shows the developed mechanical exfoliation mechanism set-up used in Graphite exfoliation.

The iron rod passing through the press roller in the exfoliation mechanism can be moved horizontally on the groove blocks, which are at the same height as the roller wall thickness and fixed to the ground on both sides of the roller. Graphite between the two-layer adhesive tape was placed on the floor so that the roller passes over the Graphite between the tapes. Graphite was separated into layers by the separation of the tapes after it was pressed with constant pressure in this set-up. Images of Graphite exfoliation process is given in Figures 2(a) and (d).

In the transfer process of Graphene onto SiO₂ frame-substrates, a mixture of acetone and isopropanol (1:2 in volume) was used to dissolve the tape's adhesive on the bottom of the Graphene samples [9]. After the adhesion between Graphene and adhesive-tape was destroyed chemically, Graphene layers were taken from the tape surface by Poly-dimethyl siloxane/ SiO₂ substrate.

A membrane layer-transfer set-up was used in the production of nanomechanical Graphene membranes on the SiO₂ frame-substrates. Graphene membranes were obtained by transferring the Graphene layers onto the frame-substrates with the help of micromanipulators in the membrane transfer mechanism set-up (in Figure 2(b)).

Transfer study was performed with micromanipulators under the digital microscope.

Membranes prepared by the transfer set-up on the frames were stretched in tension without clamps. In order to remove the liquid used in the transfer phase from the membranes, they were kept in a dust, light, and moisture-isolated desiccator containing silica gels overnight.

Characterization and tests were performed for the various acoustic pressure levels provided by a sound pressure level meter combining acoustic source and mass loads by quantum dots in various concentrations in toluene that were attached to the centers of each membrane by drop-cast method and kept in a desiccator.

3. Results and Discussion

Graphite thickness and width decrease as it exfoliates into Graphene layers [9,28,40]. The thickness of the produced membranes, determined by atomic force microscopy, was 80 ± 10 nm. The diameter, which is 1 mm with exfoliation of Graphite, decreased (Figure 2(d)) to 50 ± 15 μ m after a total of 9 exfoliations (in Figure 2(f)). Graphene membranes prepared on '10 mm \times 25 mm \times 1 mm (width \times length \times height)' size frame-pads with a 30 μ m diameter hole (in Figure 2(e)) by using the transfer mechanism is shown in Figure 2(b). Graphene membranes were examined by optical, atomic force, and scanning electron microscopies and Raman spectroscopy. Raman spectroscopy, atomic force microscopy, and optical microscopy are three techniques known to be useful for

analyzing surface morphology, disorder properties, or impurity levels of Graphene and related materials (monolayer or multilayer Graphene or Graphite layers) [9,46–49].

While the atomic force microscopy is superior to classical optical microscopes (light microscopes) in terms of examining surface morphology more closely, scanning electron microscopy is useful for analyzing molecules by approaching them more closely than the atomic force microscopes [9,46–48].

The microscope images of the Graphite crystal during exfoliation and the multi-layer suspended Graphene membrane obtained at the end of the exfoliation performed after they were transferred onto the frame-substrate are shown in Figures 2(c) and (f), respectively. As seen in the microscopy images, there are distinct differences between Graphite and Graphene (Figures 2(c) and (f)). Graphite layers have shimmer and iridescent appearance due to the light reflection coming from their thick layers (Figure 2(c)), while Graphene layers present a white-hazy appearance (Figures 2(f)) since they have more transparency with fewer layers than Graphite.

Scanning electron microscopy and atomic force microscope images of the Graphene sample images are shown in Figures 3(a) and (b). As seen in Figure 3(a), the scale-bar is 100 nm in the scanning electron microscope image.

The fact that groove-lumps with a diameter of 1-10 nm were observed on the sample surface in some places indicates that the Graphene was not fully stretched. The reason of the groove-lumps can be the pre-tension that has not been under controlled with the production setup that we have developed.

In the atomic force microscope image (Figure 3(b)), it is seen that the Graphene membrane consists of a different number of layers whose widths range between 5 μ m and 20 μ m. Since the blurry view increased as the resolution decreased, images could not be taken by getting closer to the sample. The 100 μ m scale-bar optical microscope image of the Graphene membrane (\sim 50 μ m diameter) is given in Figure 2(f).

Deformation and defect (such as irregular lattice structure) levels of the Graphene sample can be studied by Raman spectroscopy.

The presence and positions of the G-peak, D-band, D'-band and 2D-band, which are the characteristic peaks/bands of Graphene in the spectrum, can be measured by Raman spectroscopy, and information about the presence of deformation and defects can be obtained [9,46–48,50,51].

Raman spectrum of Graphene is shown in Figure 4. Raman spectrum of Graphene was measured at room temperature (25 °C) and 1% power (10 seconds integration time) by using a laser source with 532 nm excitation

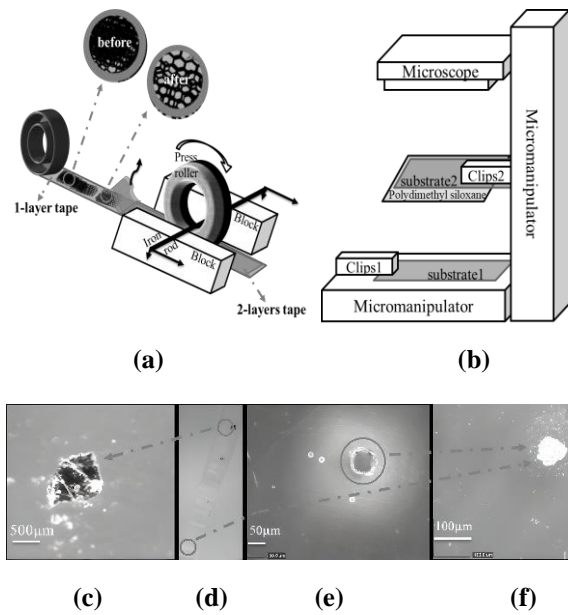


Figure 2. a) Mechanical exfoliation mechanism of graphite, b) membrane transfer mechanism, c) optical microscope image of graphite crystal, d) graphite exfoliation photo, e) optical microscope image of frame-substrate (30 μm diameter hole is marked), f) optical microscope image of graphene membrane obtained at the end of the exfoliation process on the frame-substrate (scale-bars are 500 μm in (c), 50 μm in (e) and 100 μm in (f)).

wavelength ($\lambda_{\text{excitation}}$). Laser beams scattered from Graphene were analyzed with a 50 cm focal length Raman spectrometer.

As can be seen in Figure 4, the characteristic G-peak of Graphene is at 1582 cm^{-1} , while the characteristic D-band and 2D-band are at 1335 cm^{-1} and 2719 cm^{-1} , respectively. However, the band observed in 2443 cm^{-1} is thought to be the mode named D+D" or G* and occurs due to the phonon properties of Graphene (with the contribution of the transverse optical phonon and the longitudinal acoustic phonon) [52].

In Raman spectrum of Graphene, $I_{\text{D}}/I_{\text{G}}$ value can give information about the layer number of the sample [49,53,54]. In membranes with a few numbers of layers, this value approaches zero. While $I_{\text{D}}/I_{\text{G}}$ ratio is zero for a single layer, it takes a value between 0 and 0.05 for a double layer. It also appears to have several or many layers for values between 0.05 and 0.1 and multiple layers for values between 0.1 and 0.18 [49,53,54].

In Figure 4, the $I_{\text{D}}/I_{\text{G}}$ ratio is 0.08 which can be attributed to the 'multi layers' of Graphene sample. In addition, the intensity of the 2D band of Graphene relative to the G-peak may indicate that Graphene has some irregular and imperfect lattice structure [49,53,54].

In terms of Raman spectroscopy, which is one of the useful nanometrological tools for Graphene and related materials research, it has been reported that the spectrum of Graphene also carries traces of the substrate under the

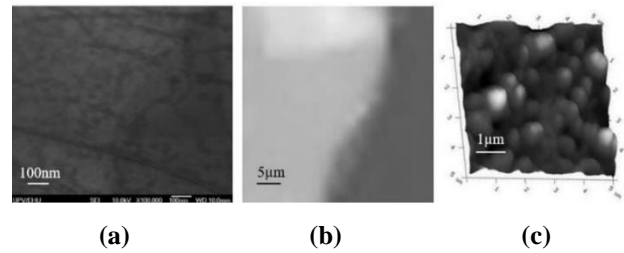


Figure 3. Images of graphene obtained from a) scanning electron microscope and b) atomic force microscope, and c) image of quantum dots from atomic force microscope (scale-bars are 100 nm in (a), 5 μm in (b), and 1 μm in (c)).

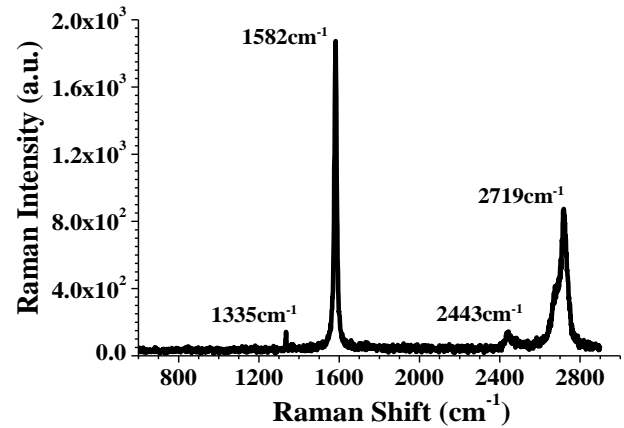


Figure 4. Raman spectrum of Graphene (a.u.: arbitrary unit) $\lambda_{\text{excitation}} = 532 \text{ nm}$.

Graphene layer together with Graphene main properties [46–48,50]. Furthermore, the type of substrate and its optical properties have a strong effect on the obtained Raman spectra [1]. SiO_2 is one of the most used materials as a Graphene substrate, and in the literature, it is known that between Graphene and SiO_2 , there are Van der Waals forces that can hold these materials together [1]. Therefore, in this study, it was not necessary to add an extra anchoring or stabilizing layer onto the Graphene membrane on the SiO_2 frame-substrate.

Determination of membrane mass loading (attached mass) capacities in ultra-low amounts and adjustable deflection responses to the acoustic signals in the human hearing frequency range (20 Hz – 20 kHz) is important in terms of using membranes as an ultra-sensitive mass sensor, pressure sensor, and acoustic sensor.

In this research, GNMs were studied in terms of their use as mass-acoustic hybrid sensors. Quantum dots, acoustic signal source, amplifier, data-logger, and laser Doppler vibrometer were used in the nanomechanical investigations of membranes. Membrane loading capacities and/or acoustic response are determined by the addition of various amounts of quantum dot materials (adjusted by concentration) to the membrane center on the membrane upper surface, and/or by the application of acoustic signal excitations (in various values and forms) at a certain distance from the lower surface of the membrane, respectively.

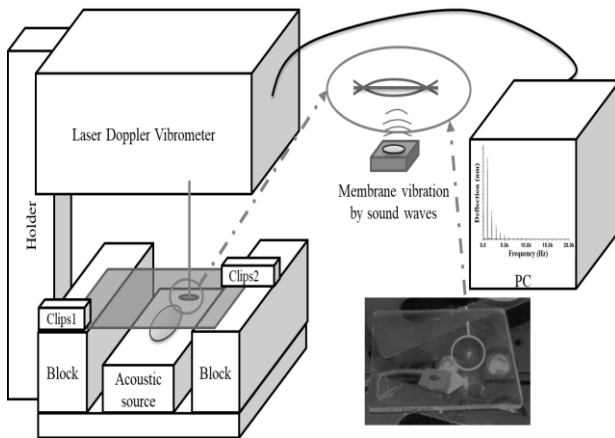


Figure 5. Deflection measurement setup.

To be able to use NMs as mass sensors, it is important to understand the response of pristine NMs and various level of mass loaded NMs under various applied sound pressure levels. In this context, while examining the loading capacities, quantum dots in toluene were diluted and prepared in different molar concentrations as mass loading sources, and measurements and evaluations were performed. The diameter of the load material (quantum dots) used in this study was 6 nm. Figure 3(c) shows a three-dimensional surface morphology of quantum dots obtained from atomic force microscopy. As seen in the microscope image, quantum dots formed closely located globular clusters with diameters ranging from 0.5 μm to 1 μm (Figure 3(c)).

The mass loading source (quantum dots in toluene) was prepared at four different molar concentrations. The stock solution was 6920 nM and diluted samples were 3190 nM, 1460 nM 730 nM and 350 nM; they were loaded into the center of four membranes in equal amounts (5 μL) by drop-casting. However, as mentioned in the literature, there is no connection between the position of the mass-load and vibration frequency [35]. Regardless of the position of the added mass, the vibration frequency decreases as the attached mass increases [35].

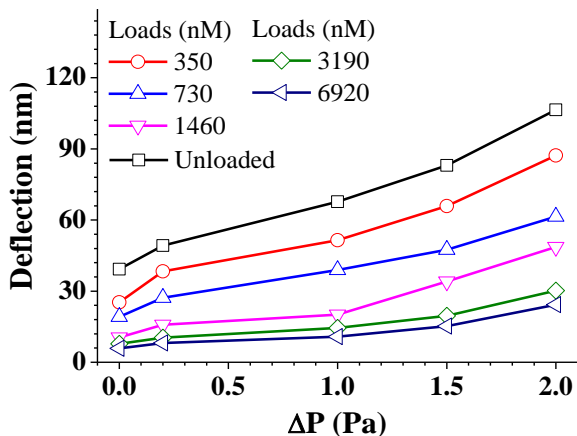
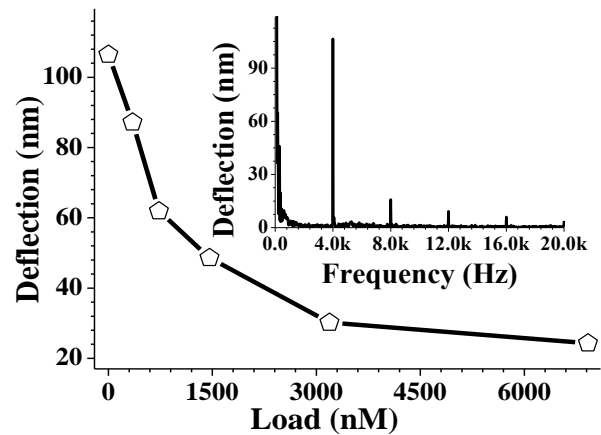
Figure 6. Deflection of membrane with the added mass loads for applied pressure differences (ΔP) up to 2 Pa.

Figure 7. Membrane deflection dependency with mass loads under 2 Pa. Inset figure shows the mechanic resonance spectrum of unloaded membrane under 2 Pa.

After the casting processes, samples were kept in a sealed container for a night to remove toluene from quantum dots and the membrane surface.

The image of the set-up used in nanomechanical deflection measurements is shown in Figure 5 where an acoustic source and a laser Doppler vibrometer are placed 10 mm below and 50 cm above the GNM sample, respectively. The laser point of the Doppler vibrometer was adjusted onto the middle of the membrane. Detection and processing of acoustic responses of the NMs were studied by examining membrane deflection amplitudes with the applied acoustic signal excitations up to 2 Pa in the human hearing frequency range.

Figure 6 shows the deflection characteristics of pristine (unloaded) and centrally mass loaded Graphene membranes, which vary according to the applied acoustic pressure differences values up to 2 Pa. A change in the mass attached to the NM caused a change in the amount of deflection. The deflection values for all membrane samples increased as the applied pressure increased from 0.02 Pa to 2 Pa. Membrane deflection dependency with the mass loads under 2 Pa is shown in Figure 7.

Under the constant pressure of 2 Pa, membrane deflection decreases as the mass load increases. Based on Equation (1), it can be said that deflection is inversely proportional to the thickness [11]. The reason why the mass load is inversely proportional to the membrane deflection is that the thickness increases with the mass load since the mass load is placed on the center of each membrane [11].

The NM mass includes the membrane's own mass and the attached mass. According to Equations (1) and (2), as mass loads increase, membrane thickness increases, whereas membrane deflection and membrane vibration frequency decrease. Regarding Equations (2) and (3), it can be said that because the high mass sensitivity membranes show high mass-detection resolution, the sensitivity is high in membranes with low mass and high vibration frequency.

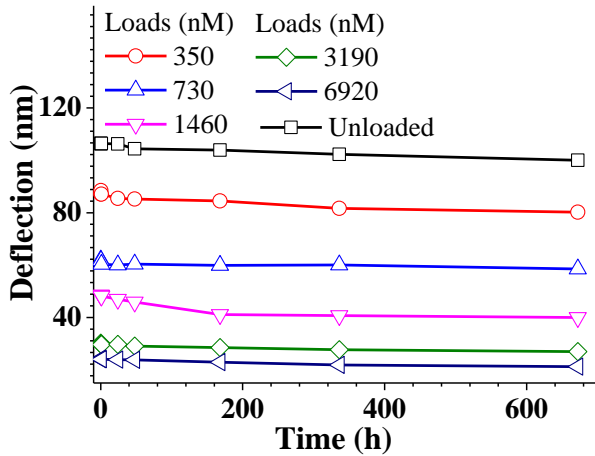


Figure 8. Membrane deflection dependencies in time under 2 Pa.

In the frequency-dependent deflection characteristics of the unloaded membrane at 2 Pa (inset of Figure 7), the membrane has the main peak at 4 kHz (4 kHz is in the speaking frequency bandwidth) in correlation with the source frequency. In addition, periodic harmonic signal peaks are visible at 8 kHz, 12 kHz, 16 kHz, and 20 kHz frequencies that can be attributed to the presence of degenerate modes mediated by the membrane surface contamination, membrane asymmetries in the stress profile, or membrane degeneration [44].

Based on the experiments, it can be said that the most sensitive Graphene membrane sample was the unloaded NMM with 67.8 ± 5 nm/Pa. Although the membrane acoustic sensitivity increases as the membrane area increases [14], $706.5 \mu\text{m}^2$ area Graphene NMMs produced in this study have more sensitivity than the commercial $\sim 708462.5 \mu\text{m}^2$ area microphone membranes that have sensitivities around 3 nm/Pa (like STMicroelectronics purple pentagon MP23DB01HP, MP34DT04 type products) [14].

In the context of the study, time-dependent deflection dependency analysis was carried out to analyze the membrane durability. Figure 8 shows deflection dependency characteristics of the GNM over time up to 1 month under 2 Pa. All NMs show a slight decrease in their deflection characteristics over time.

4. Current Challenges and Future Prospects of Nanomechanical Sensors

GNMs have many challenges, both economically and technically.

Regarding the economic challenges, the NM sensor device preparation method is a big challenge. Whereas the low-cost and facile mechanical exfoliation method (top-down technique) gives limited-area (several tens of microns) layers, the higher-cost and more complex CVD method (bottom-up technique) can give high quality large-area layers.

Regarding the technical challenges, device durability can

be shown as one of the challenges of the NMs. Although Graphene layers/membranes have resistance against air, moisture, humidity, or chemical, suspended GNM deflection durability can decrease over time.

GNMs can find application in futuristic areas like spintronics or magneto-inductive signal generation as simple molecular machines or sensors. For instance, in a study, Graphene as an NM was used as a damped vibrating system with single-molecule magnet materials (like Terbium(iii) bis-phthalocyanines) attached to the Graphene membrane to work as a THz signal source of significantly lower complexity compared to complex THz integrated circuits [43]. Such single-molecule magnets are highly compatible with Graphene membranes for spintronics applications [7,10]. Therefore, GNM systems are promising as new forms of magneto-inductive and THz signal generation as simple molecular machines or sensors, and they will further enhance the future capabilities of quantum nanomachines and sensor systems with their quantum mechanical properties [7,10,43]. With the fully nanomechanical stand-alone membrane-based sensor system studied in this article, nanoscale mass and acoustic sensing in vitro systems for wearable smart electronics and healthcare applications (such as accelerometers, molecular machines, or microfluidics) can be realized. Accelerometers and microphones are widely used healthcare sensors for vibration and acoustic signal sensing, respectively [55].

Some features such as low mass, large surface area, elasticity, high sensitivity to small mass loading, and sound frequency make GNMs ideal for use in the healthcare applications as acoustic, force, and load sensors for wearable or tracking/laboratory analysis [26,56–58]. GNMs have been in development since 2007 and still receive significant attention in laboratory research in the academic field. The continued interest in GNM devices is due to their easy and cost-effective manufacturing methods, wide variety of applications, and commercial successes. To further develop these GNM sensor devices, their future work needs to be aligned with industry requirements.

5. Conclusions

In this study, the mass and acoustic response of suspended multilayer GNMs for sensor applications that can be used for the healthcare industry was investigated. GNM sensors were produced, morphologically and spectroscopically characterized, and analyzed in the air at room temperature with various attached mass loads and acoustic pressure levels. It was determined that the sensitivity obtained from the produced $706.5 \mu\text{m}^2$ area membranes was highest at 67.8 ± 5 nm/Pa, which can be comparable with the commercial ones. NMs, are presented in this article can provide benefits in terms of producing facile, low-cost low-mass, non-destructive and practical GNM-based masses, pressure and acoustic sensors that can be useful as micro-sensors,

transducers or molecular machines in biomedical, and environmental monitoring or microfluidic applications.

In terms of the NMs with low material and production costs, and sensitivity and durability of the NMs that can compete with the previous studies reported in the literature (Table 1), some important points of the study are highlighted below:

- Production of GNMs on low-cost SiO₂ frame-substrate using exfoliation method (without extra stabilizing layer addition or no requirement of high vacuum and chemical gas).
- No energy consumption for the removal of humidity from the NMs (no necessity to use an oven or vacuum-oven).
- Similar membrane thicknesses at the end of each exfoliation process thanks to the developed membrane exfoliation set-up (can be developed further by an automatization through the roll-to-roll process).
- The wet-coating technique (drop-casting) to prepare loaded-membranes (instead of high-cost evaporation like vacuum-thermal coating).
- Membrane vibrational deflection measurements with optical reading at room temperature and in the open atmosphere (low temperature under vacuum in literature).
- Easily accessible and comfortable measurement conditions (in the air at room temperature).
- High detectivity in the air at room temperature by the developed membrane deflection measurement set-up.
- For the air, temperature, and humidity stable sensors, encapsulation techniques can be used to get better NM deflection durability over time.

In the mechanical exfoliation process, Graphite gets thinner by dividing into layers at each stage. The problem related to this process is that as the Graphite gets thinner, its width also decreases. The solution to this problem may be the use of highly oriented Graphite: thinner and wider-area membranes can be produced by using highly oriented Graphite instead of Graphite crystal as the main source of Graphene.

Mechanical exfoliation and the performance of the membrane transfer mechanisms are crucial to get similar results on the membrane diameter. Therefore, low-area NM sensors with green production methods can be developed by further improving the membrane exfoliation set-up (e.g., the manual roll-to-roll process, where the adhesive tape is bent and peeled by the rolls automatically, can be connected to the exfoliation mechanism).

Another possible performance improvement option may be using the CVD (although it requires high energy consumption) for the membrane preparation to prepare large-area membranes. Finally, sensor performance can be further improved by using higher-quality Graphite sources such as highly oriented Graphite, which can be more expensive than the Graphite crystal used in this study for the mechanical exfoliation process.

Declaration

The author declared no potential conflicts of interest with respect to the research, authorship, and/or publication of this article. The author also declared that this article is original, was prepared in accordance with international publication and research ethics, and ethical committee permission or any special permission is not required.

Author Contributions

G. Memisoglu developed the methodology, performed the analysis, improved the study and wrote the manuscript.

Acknowledgment

The author acknowledges the project support funds of the European Union's H2020 Marie Skłodowska Curie Multiply Research Project No 713694. Author would like to thank Dr. J. Villatoro, Dr. J. Zubia and Dr. A. Rozhin for providing laboratory facilities, Dr. R. Fernandez, Dr. M. Azkune and Dr. R. Montero for the technical supports.

Nomenclature

<i>GNM</i>	: Graphene-based nanomechanical membrane
<i>GM</i>	: Graphene-based membrane
<i>NM</i>	: Nanomechanical membrane
<i>SiO₂</i>	: Silicon dioxide
<i>CdS</i>	: Cadmium sulphide
<i>CVD</i>	: Chemical vapor deposition
$\lambda_{excitation}$: Excitation wavelength
$m_{attached}$: Attached mass (loaded mass)
$f_{withoutmass}$: Vibration frequency of pristine membrane
$f_{withmass}$: Vibration frequency of membrane with mass
$\alpha_{i,j}$: Dimensionless parameter
r	: Membrane radius
T	: Membrane tension
ρ	: Membrane density
t	: Membrane thickness
$m_{effective}$: Effective mass
R_{mass}	: Mass responsivity

References

1. Bunch, J.S., et al., *Electromechanical Resonators from Graphene Sheets*. Science, 2007. **315**: p. 490–493.
2. Chen, C., et al., *Performance of Monolayer Graphene Nanomechanical Resonators with Electrical Readout*. Nature Nanotechnology, 2009. **4**: p. 861–867.
3. Zhou, X., et al., *The Rise of Graphene Photonic Crystal Fibers*. Advanced Functional Materials, 2022. **32**(42): p. 2202282.
4. Novoselov, K.S., et al., *Electric Field Effect in Atomically Thin Carbon Films*. Science, 2004. **306**: p. 666–670.
5. Shin, D.H., et al., *Graphene Nano-Electromechanical Mass Sensor with High Resolution at Room Temperature*. iScience, 2023. p. 1059
6. Cakmak, N.K., Kucukyazici, M., Eroglu, A., *Synthesis and stability analysis of folic acid-graphene oxide nanoparticles for drug delivery and targeted cancer therapies*. International Advanced Researches and Engineering Journal, 2019. **3**(2): p. 81-85.

7. Cervetti, C., et al. *The Classical and Quantum Dynamics of Molecular Spins on Graphene*. Nature Materials, 2016. **15**: p. 164–168.
8. Ferrari, A.C., et al., *Science and Technology Roadmap for Graphene, Related Two-Dimensional Crystals, and Hybrid Systems*. Nanoscale, 2015. **7**: p. 4598–4810.
9. Memisoglu, G., Gulbahar, B., Fernandez-Bello, R., *Preparation and Characterization of Freely-Suspended Graphene Nanomechanical Membrane Devices with Quantum Dots for Point-of-Care Applications*. Micromachines, 2020. **11**: p. 1–14.
10. Stickler, B.A., and Hornberger, K., *Molecular Rotations in Matter-Wave Interferometry*. Physical Review A - Atomic, Molecular, and Optical Physics, 2015. **92**: p. 1–8.
11. Bunch, J.S., et al., *Impermeable Atomic Membranes from Graphene Sheets*. Nano Letters, 2008. **8**: p. 2458–2462.
12. Chen, C., et al., *Graphene Mechanical Oscillators with Tunable Frequency*. Nature Nanotechnology, 2013. **8**: p. 923–927.
13. Imamura, G., et al., *Graphene Oxide as a Sensing Material for Gas Detection based on Nanomechanical Sensors in the Static Mode*. Chemosensors, 2020. **8**: p. 1–17.
14. Pezone, R., et al., *Sensitive Transfer-Free Wafer-Scale Graphene Microphones*. ACS Applied Materials and Interfaces, 2022.
15. Standley, B., Bao, W., Zhang, H., Bruck, J., *Graphene-Based Atomic-Scale Switches*. Nano Letters, 2008. **8**: p. 3345–3349.
16. Wu, Z.S., Parvez, K., Feng, X., Müllen, K., *Graphene-Based in-Plane Micro-Supercapacitors with High Power and Energy Densities*. Nature Communications, 2013. **4**.
17. Akyildiz, I.F., and Jornet, J.M. *The Internet of Nano-Things*. IEEE Wireless Communications, 2010. **17**: p. 58–63.
18. Akyildiz, I.F.; Jornet, J.M. *Electromagnetic Wireless Nanosensor Networks*. Nano Communication Networks, 2010, **1**: p. 3–19.
19. Rogers, J., Huang, Y., Schmidt, O.G., Gracias, D.H., *Origami MEMS and NEMS*. MRS Bulletin, 2016. **41**: p. 123–129.
20. Chen, Y., Zhang, B., Liu, G., Zhuang, X., Kang, E.T., *Graphene and Its Derivatives: Switching on and Off*. Chemical Society Reviews, 2012. **41**: p. 4688–4707.
21. Memisoglu, G., and Gulbahar, B. *Supercapacitor Assembly for Portable Electronic Devices, and Method of Operating the Same*, EPO Patent - EP003422376B1, 2021. p. 1–12.
22. Shiba, K., et al., *Functional Nanoparticles-Coated Nanomechanical Sensor Arrays for Machine Learning-Based Quantitative Odor Analysis*. ACS Sensors, 2018. **3**: p. 1592–1600.
23. Memisoglu, G., and Gulbahar, B. *Acousto - Optic Transducer Array and Method*, US Patent - US20200068318A1, 2020: p. 1–5.
24. Zande, A.M.V.D., et al., *Large-Scale Arrays of Single Layer Graphene Resonators*, Nano Letters, 2010. **10**(12): p. 4869–4873.
25. Ma, J., Jin, W., Ho, H.L., Dai, J.Y. *High-Sensitivity Fiber-Tip Pressure Sensor with Graphene Diaphragm*. Optics Letters 2012. **37**: p. 2493.
26. Gulbahar, B., and Memisoglu, G. *CSSTag: Optical Nanoscale Radar and Particle Tracking for In-Body and Microfluidic Systems with Vibrating Graphene and Resonance Energy Transfer*. IEEE Transactions on Nanobioscience, 2017. **16**(8), p. 905–916.
27. Adhikari, S., Chowdhury, R. *Zeptogram Sensing from Gigahertz Vibration: Graphene based Nanosensor*. Physica E, 2012. **44**: p. 1528–1534.
28. Memisoglu, G. *Vibrating FRET based Nanomechanical Sensor Preparation and Characterization for Environmental Monitoring Applications*. IEEE Sensors Journal, 2021. **21**: p. 3871–3878.
29. Liu, S., et al., *Nano-Optomechanical Resonators based Graphene/Au Membrane for Current Sensing*. Journal of Lightwave Technology, 2022. **40**: p. 7200–7207.
30. Liu, S., et al., *Nano-Optomechanical Resonators based on Suspended Graphene for Thermal Stress Sensing*. Sensors, 2022. **22**: p. 9068.
31. Singh, V., et al., *Probing Thermal Expansion of Graphene and Modal Dispersion at Low-Temperature Using Graphene Nanoelectromechanical Systems Resonators*. Nanotechnology, 2010. **21**: p. 165204.
32. Gulbahar, B., and Memisoglu, G. *Nanoscale Optical Communications Modulator and Acousto-Optic Transduction with Vibrating Graphene and Resonance Energy Transfer*. In Proceedings of the IEEE International Conference on Communications, 2017.
33. Chen, T., et al., *Designing Energy-Efficient Separation Membranes: Knowledge from Nature for a Sustainable Future*. Advanced Membranes, 2022. **2**: p. 100031.
34. Gupta, A., Sakthivel, T., Seal, S. *Recent Development in 2D Materials beyond Graphene*. Progress in Materials Science, 2015. **73**: p. 44–126.
35. Duan, K., Li, L., Hu, Y., Wang, X., *Pillared Graphene as an Ultra-High Sensitivity Mass Sensor*. Scientific Reports, 2017. **7**: p. 1–8.
36. Fletcher, N. *Acoustic Systems in Biology*; New York: Oxford University Press, Inc., 1992.
37. Ekinci, K.L., Yang, Y.T., Roukes, M.L., *Ultimate Limits to Inertial Mass Sensing based upon Nanoelectromechanical Systems*. Journal of Applied Physics, 2004. **95**: p. 2682–2689.
38. Liu, Y., Dong, X., Chen, P., *Biological and Chemical Sensors Based on Graphene Materials*. Chemical Society Reviews, 2012. **41**: p. 2283–2307.
39. Sakhaee-Pour, A., and Ahmadian, M.T., Vafai, A. *Applications of Single-Layered Graphene Sheets as Mass Sensors and Atomistic Dust Detectors*. Solid State Communications, 2008. **145**: p. 168–172.
40. Castellanos-Gomez, A., et al., *Deterministic Transfer of Two-Dimensional Materials by All-Dry Viscoelastic Stamping*. 2D Materials, 2014. **1**: p. 1–34.
41. Frisenda, R., et al., *Recent Progress in the Assembly of Nanodevices and van Der Waals Heterostructures by Deterministic Placement of 2D Materials*. Chemical Society Reviews, 2018. **47**: p. 53–68.
42. Smith, A.D., et al., *Piezoresistive Properties of Suspended Graphene Membranes under Uniaxial and Biaxial Strain in Nanoelectromechanical Pressure Sensors*. ACS Nano, 2016. **10**: p. 9879–9886.
43. Gulbahar, B. *Energy Harvesting and Magneto-Inductive Communications with Molecular Magnets on Vibrating Graphene and Biomedical Applications in the KHz to THz Band*. IEEE Transactions on Molecular, Biological, and Multi-Scale Communications, 2017. **3**: p. 194–206.
44. Barton, R.A., et al., *High, Size-Dependent Quality Factor in*

- an Array of Graphene Mechanical Resonators*. Nano Letters, 2011. **11**: p. 1232–1236.
45. Chen, Y., et al., *Nano-Optomechanical Resonators for Sensitive Pressure Sensing*. ACS Applied Materials and Interfaces, 2022. **14**: p. 39211–39219.
 46. Ferrari, A.C., *Raman Spectroscopy of Graphene and Graphite: Disorder, Electron-Phonon Coupling, Doping and Nonadiabatic Effects*. Solid State Communications, 2007. **143**: p. 47–57.
 47. Ferrari, A.C., et al., *Raman Spectrum of Graphene and Graphene Layers*. Physical Review Letters, 2006. **97**: p. 1–4.
 48. Ferrante, C., et al., *Raman Spectroscopy of Graphene under Ultrafast Laser Excitation*. Nature Communications 2018. **9**: p. 1–8.
 49. Tahir, N.A.M., et al., *Optimisation of Graphene Grown from Solid Waste Using CVD Method*. International Journal of Advanced Manufacturing Technology, 2020. **106**: p. 211–218.
 50. Eckmann, A., et al., *Probing the Nature of Defects in Graphene by Raman Spectroscopy*. Nano Letters, 2012. **12**: p. 3925–3930.
 51. Calizo, I., Balandin, A.A., Bao, W., Miao, F., Lau, C.N., *Temperature Dependence of the Raman Spectra of Graphene and Graphene Multilayers*. Nano Letters, 2007. **7**: p. 2645–2649.
 52. May, P., et al., *Signature of the Two-Dimensional Phonon Dispersion in Graphene Probed by Double-Resonant Raman Scattering*. Physical Review B - Condensed Matter and Materials Physics, 2013. **87**.
 53. Alshaikh, M.M., *Mica as an Ultra-Flat Substrate for Studying Mechanically Exfoliated Graphene*, Swansea University, 2021.
 54. *Instantano Graphene Number of Layers Calculator From ID/IG and I2D/IG Ratio via Raman Spectroscopy* Available online:
<https://instantano.com/characterization/calculator/raman/graphene-layers/>.
 55. Mallegni, N., et al., *Sensing Devices for Detecting and Processing Acoustic Signals in Healthcare*. Biosensors, 2022. **12**: p. 835.
 56. Memisoglu, G., Gulbahar, B., Zubia, J., Villatoro, J., *Theoretical Modeling of Viscosity Monitoring with Vibrating Resonance Energy Transfer for Point-of-Care and Environmental Monitoring Applications*. Micromachines, 2018. **10**: p. 11.
 57. Sachdeva, A., Singh, P.K., Rhee, H.W. *Composite Materials Properties, Characterization, and Applications*; Amit Sachdeva, Pramod Kumar Singh, H.W.R., Ed.; CRC Press, Taylor and Francis Group, 2021. ISBN 978-1-003-08063-3.
 58. Zhang, H., et al., *Graphene-Enabled Wearable Sensors for Healthcare Monitoring*. Biosensors and Bioelectronics, 2022. **197**: p. 11–13.